Journal of ELECTRONIC MATERIALS, Vol. 37, No. 11, 2008
DOI: 10.1007/s11664-008-0536-y

Regular Issue Paper

Improved Uniformity and Electrical Performance of Continuous-Wave Laser-Crystallized TFTs Using Metal-Induced Laterally Crystallized Si Film

CHIH-PANG CHANG[1] and YEWCHUNG SERMON WU[1,2]

1.—Department of Materials Science and Engineering, National Chiao Tung University, Hsinchu 300, Taiwan, Republic of China. 2.—e-mail: SermonWu@Stanfordalumni.org

Continuous-wave (CW) laser crystallization (CLC) of amorphous Si (α-Si) has previously been employed to fabricate high-performance low-temperature polycrystalline silicon (poly-Si) thin-film transistors (TFTs). Unfortunately, their uniformity was poor because the shape of the beam profiles was Gaussian. In this study, α-Si film was replaced by Ni-metal-induced laterally crystallized Si (MILC-Si). MILCLC-Si was MILC-Si irradiated by a CW laser ($\lambda \approx 532$ nm and power ≈ 3.8 W). It was found that the performance and uniformity of the metal-induced laterally crystallized continuous-wave laser crystallization - thin film transistors (MILCLC-TFTs) were much better than those of the CLC-TFTs. Therefore, the MILCLC-TFT is suitable for application in systems on panels.

Key words: Metal-induced lateral crystallization, continuous-wave laser, polycrystalline-silicon thin-film transistors

INTRODUCTION

Low-temperature polycrystalline silicon (LTPS) thin-film transistors (TFTs) have attracted considerable interest for their application in organic light-emitting diode displays and liquid-crystal displays, since they exhibit good electrical properties and can be integrated into peripheral circuits on inexpensive glass substrates.[1] For the application to systems on panels (SOP) and solar cells, the uniformity of polycrystalline silicon (poly-Si) grain size and crystallinity should be improved.

As LTPS TFTs require glass substrates, intensive studies on reducing the crystallization temperature of amorphous silicon (α-Si) films have thus been carried out. Ni-metal-induced lateral crystallization (MILC) is one of these efforts. In MILC, Ni islands are selectively deposited on top of α-Si films and allowed to crystallize at a temperature below 600°C.[2,3] Continuous-wave (CW) laser crystallization (CLC) of α-Si has also been recently employed to fabricate high-performance LTPS TFTs.[4–7] Compared with the excimer laser crystallization (ELC) process, the CLC process is simpler, easier, and relatively inexpensive. Unfortunately, the resulting uniformity was poor because the shape of the beam profiles was Gaussian.[8]

To improve the uniformity of CLC-TFT, a new method for fabricating metal-induced laterally crystallized continuous-wave laser crystallization - thin film transistors (MILCLC-TFTs) is proposed in this letter. Instead of α-Si, MILC-Si film was irradiated by a CW laser at various output powers.

EXPERIMENT

Two kinds of Si films (α-Si and MILC-Si) were irradiated by CW laser at room temperature in an air atmosphere. Samples designated "CLC" were α-Si films and those designated "MILCLC" were MILC-Si films irradiated by CW laser. A 4-inch quartz wafer with a 500-nm-thick wet oxide layer was used as the substrate. To form the α-Si film, a 100-nm-thick silane-based undoped α-Si layer was deposited using low-pressure chemical vapor deposition (LPCVD). To

---

(Received June 11, 2008; accepted July 28, 2008;

form the MILC-Si film, Ni lines were deposited on the α-Si film and subsequently annealed at 550°C for 12 h.[9] Both films were then irradiated using a CW laser at various output powers (2.5 W, 3.8 W, and 5 W). When fabricating the MILCLC poly-Si, the scanning direction of the CW laser was parallel to the MILC needle-like poly-Si grains.

Reactive ion etching (RIE) was employed to form islands of poly-Si regions on the wafers. Next, a 100-nm-thick tetraethylorthosilicate/O_2 oxide layer was deposited as the gate insulator by plasma-enhanced chemical vapor deposition (PECVD). Then a 200-nm-thick poly-Si film was deposited as the gate electrode by LPCVD. After defining the gate, self-aligned 40-keV phosphorous ions were implanted at a dose of 5×10^{15} cm^{-2} to form the source/drain and gate. Dopant activation was performed at 600°C in N_2 ambient for 24 h. Contact holes were formed and a 500-nm-thick Al layer was then deposited by thermal evaporation and patterned as the electrode. The sintering process was performed at 400°C for 30 min.

RESULTS AND DISCUSSION

Figure 1 shows scanning electron microscopy (SEM) images of the Secco-etched CLC and MILCLC irradiated under various laser output powers. As can be seen, the CLC poly-Si comprises grains of various sizes distributed in three distinct regions.[8] As shown in Fig. 1a, at the laser output power of 2.5 W, CLC-2.5 was found to be in the solid phase crystallization (SPC) region with fine grains. With increasing laser output power, CLC-3.8 was found to be in the partially melted region with large ELC poly-Si-like grains, as shown in Fig. 1b.[8] When the laser output power reached 5.0 W, CLC-5.0 was found to be in the completely melted region. As seen in Fig. 1c, the uniformity of CLC-5.0 grains was poor, containing both ELC poly-Si-like grains and very large directional grains.

As for the fabrication of the MILCLC poly-Si, Fig. 1d shows that, at lower laser output power, the sizes and shapes of MILCLC-2.5 needle Si grains were similar to those of MILC poly-Si. This is because MILCLC-2.5 was found to be in the SPC region. Only some of the α-Si regions among the Si grains were melted and crystallized. When the laser output power reached 3.8 W, the width of the MILCLC-3.8 grains increased to 3 μm, as shown in Fig. 1e. Compared with that of CLC-3.8, the grain size of MILCLC-3.8 was larger and the uniformity was better. We believe that most of the α-Si and small MILC grains in this regime were molten. However, the large grains were only partially molten and served as predetermined nuclei for grain growth. The width of these grains increased markedly due to the geometrical coalescence of Si needle grains. Geometrical coalescence can be simply described as an encounter of grains whose relative orientations are similar during grain growth.[10] The grain boundary between grains disappears, resulting in sudden development of a much larger grain. This coalescence is an important phenomenon for grains having a strong preferred orientation. In this study, MILC needle Si grains had a strong preferred orientation of ⟨111⟩.

The crystal structure of MILCLC-5.0 was similar to that of CLC-5.0. It contained both ELC

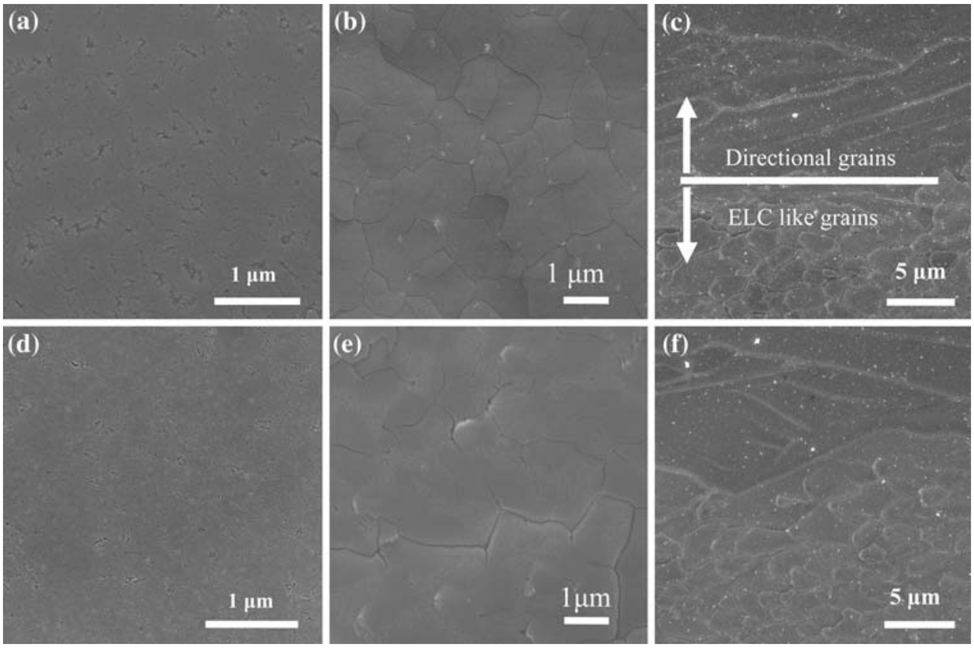

Fig. 1. SEM images of Secco-etched poly-Si grains irradiated by CW laser with various powers: (a) CLC-2.5, (b) CLC-3.8, (c) CLC-5.0, (d) MILCLC-2.5, (e) MILCLC-3.8, and (f) MILCLC-5.0.

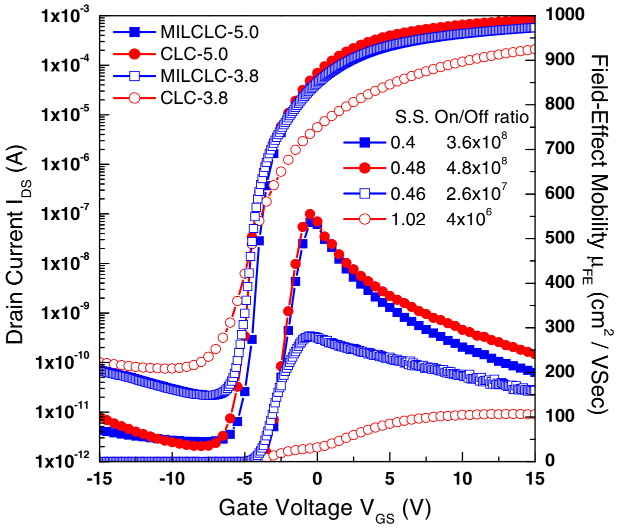

Fig. 2. Typical I_{DS}–V_{GS} transfer characteristics and field-effect motilities of MILCLC and CLC TFTs (W/L = 20 μm/20 μm).

poly-Si-like grains and very large directional grains. As shown in Fig. 1f, the uniformity of MILCLC-5.0 grains was poor. This is because MILCLC-5.0 was found to be in the completely melted region.

Figure 2 shows the transfer characteristics and field-effect mobility versus the gate voltage of TFTs in the random grain structure for $W = L = 20\ \mu$m at V_{DS} = 5 V and V_{DS} = 0.1 V, respectively. The measured and extracted key device parameters are also summarized in Fig. 2. The threshold voltage (V_{th}) was defined as the gate voltage required to achieve a normalized drain current of $I_{DS} = (W/L) \times 100$ nA at V_{DS} = 5 V. It was found that, when the laser output power was 5.0 W, the electrical performance of MILCLC-5.0 and CLC-5.0 was similar, both showing excellent performance. This is because they were in the completely melted region. Both Si films had very large directional grains.

However, the performance of MILCLC-3.8 and CLC-3.8 TFTs were quite different when the laser output power was 3.8 W. Compared with CLC-3.8 TFTs, MILCLC-3.8 TFTs exhibited higher field-effect mobility, superior subthreshold slope (SS), lower threshold voltage (V_{th}), and higher on/off current ratio. The superior performance of MILCLC-3.8 is attributed to the quality of large silicon grains. As seen in Fig. 1e, the size of MILCLC-3.8 coalescence grains was larger than that of CLC-3.8 grains. Moreover, most of these coalescence grains and their boundaries were parallel to the drain current (I_{DS}), which reduced the impedance to carrier flow. This in turn decreased the threshold voltage and increased greatly the mobility and I_{on}/I_{off} current ratio.

The electrical characteristics of both CLC-2.5 and MILCLC-2.5 were not as good as those of other TFTs. The performance of CLC-2.5 TFT was similar to that of SPC since the CLC-2.5 film contained SPC poly-Si-like grains. On the other hand, the performance of MILCLC-2.5 TFT was similar to that of MILC-Si since only some of the α-Si regions among MILC grains were melted. As a result, the mobility of CLC-2.5 was 4.1 cm^2/V s, while that of MILCLC-2.5 was 50 cm^2/V s. [11]

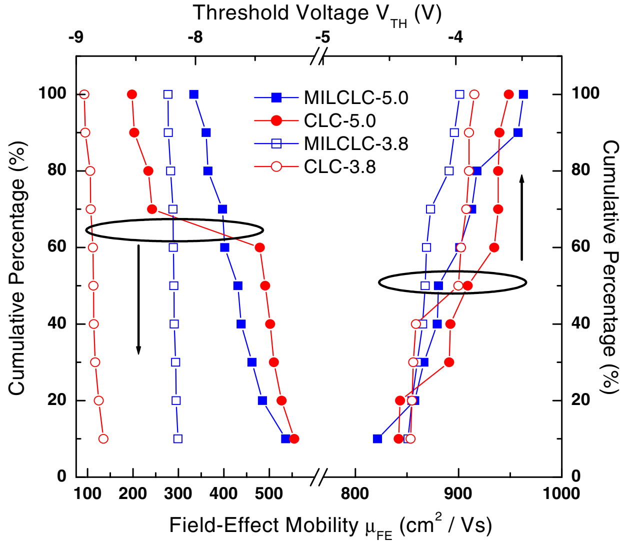

Fig. 3. The field-effect mobility and threshold voltage of ten TFTs were measured in each case to investigate device-to-device variation.

Table I. Average Values of the Field-Effect Mobility and Threshold Voltage of Two Different Structures (Standard Deviations in Parentheses)

TFT ($W = L$ = 20 μm)	Field-Effect Mobility (cm^2/V s) μ_{FE}	Threshold Voltage (V) V_{th}
MILCLC-5.0	421 (62)	−4 (0.34)
CLC-5.0	394 (152)	−3.9 (0.31)
MILCLC-3.8	288 (7.2)	−4.19 (0.13)
CLC-3.8	112 (13)	−4.08 (0.21)

The other important issue of poly-Si TFTs is their uniformity for application on SOP and solar cells. As shown in Fig. 3, ten TFTs were measured in each case to investigate the device-to-device variation. Table I lists the average values of the field-effect mobility and threshold voltage of TFTs with standard deviations in parentheses. Since the electrical characteristics of CLC-2.5 and MILCLC-2.5 were poor, their uniformities were not listed here. Although the mobility of both MILCLC-5.0 and CLC-5.0 was high, their uniformity was poor and their standard deviations were large. This is because both films contained two different kinds of grains: ELC poly-Si-like grains and very large directional grains. The uniformity of CLC-3.8 and MILCLC-3.8 was much better and their standard deviations were small. As mentioned previously, MILCLC-3.8 has uniformly distributed geometrical coalescence grains. As a result, MILCLC-3.8 has the smallest standard deviation.

CONCLUSION

To improve the uniformity and electrical performance of CLC-TFTs, two kinds of Si films (α-Si and MILC-Si) were used in this study. After irradiation by a CW laser at various output powers (2.5 W, 3.8 W, and 5 W), it was found that the performance and uniformity of MILCLC-TFTs were better than those of CLC-TFTs. When the laser output power was low (2.5 W), both films were found to be in the SPC region. Only some of the α-Si regions were melted. The electrical characteristics of CLC-2.5 and MILCLC-2.5 were poor. When the laser output power reached 5.0 W, CLC-5.0 and MILCLC-5.0 were found to be in the completely melted region. They both showed excellent performance. Unfortunately, the uniformity was poor because they contained two kinds of grains: ELC poly-Si-like grains and very large directional grains. When the laser output power was intermediate (3.8 W), CLC-3.8 and MILCLC-3.8 were found to be in the partially melted region with large ELC poly-Si-like grains. The performance and uniformity of MILCLC-3.8 were much better than those of CLC-3.8. This is because the width of the MILCLC-3.8 grains increased dramatically due to the geometrical coalescence of MILC-Si needle grains. Moreover, the uniformity of MILCLC-3.8 was far superior to that of CLC-5.0 and MILCLC-5.0, and therefore was suitable for SOP application.

ACKNOWLEDGEMENTS

This project was funded by Sino American Silicon Products Incorporation and the National Science Council of the Republic of China under Grant Nos. 95-2221-E009-087-MY3. Technical supports from the National Nano Device Laboratory, the Center for Nano Science and Technology, and the Nano Facility Center of the National Chiao Tung University are also acknowledged.

REFERENCES

1. M. Stewart, R.S. Howell, L. Pires, and M.K. Hatalis, *IEEE Trans. Electron. Dev.* 48, 845 (2001). doi:10.1109/16.918227.
2. S.W. Lee and S.K. Joo, *IEEE Electron. Dev. Lett.* 17, 160 (1996). doi:10.1109/55.485160.
3. Z. Meng, M. Wang, and M. Wong, *IEEE Trans. Electron. Dev.* 47, 404 (2000). doi:10.1109/16.822287.
4. A. Hara, M. Takei, F. Takeuchi, K. Suga, K. Yoshino, M. Chida et al., *Jpn. J. Appl. Phys.* 43, 1269 (2004). doi:10.1143/JJAP.43.1269.
5. A. Hara, K. Yoshino, F. Takeuchi, and N. Sasaki, *Jpn. J. Appl. Phys.* 42, 23 (2004). doi:10.1143/JJAP.42.23.
6. Y.T. Lin, C. Chen, J.M. Shieh, Y.J. Lee, C.L. Pan, C.W. Cheng et al., *Appl. Phys. Lett.* 88, 233511 (2006). doi:10.1063/1.2209198.
7. Y.T. Lin, C. Chen, J.M. Shieh, Y.J. Lee, and C.L. Pan, *Appl. Phys. Lett.* 90, 073508 (2007). doi:10.1063/1.2644927.
8. S.J. Park, S.H. Kang, Y.M. Ku, and J. Jang, *Mat. Res. Soc. Symp. Proc.* 814, I2.3.1/A3.3.1 (2004).
9. C.M. Hu, Y.S. Wu, and C.C. Lin, *IEEE Electron. Dev. Lett.* 28, 1000 (2007). doi:10.1109/LED.2007.907267.
10. E. Robert, R. Hill, and R. Abbaschian, *Physical Metallurgy Principles*, 3rd ed. (Boston: Thomson, 1992), p. 254.
11. C.W. Chao, Y.S. Wu, G.R. Hu, and M.S. Feng, *Jpn. J. Appl. Phys.* 42, 1556 (2003). doi:10.1143/JJAP.42.1556.